ELSEVIER

Polymer 43 (2002) 3785–3793

polymer

www.elsevier.com/locate/polymer

Rheology, phase morphology, mechanical, impact and thermal properties of polypropylene/metallocene catalysed ethylene 1-octene copolymer blends

T. McNally[a,*], P. McShane[a], G.M. Nally[b], W.R. Murphy[b], M. Cook[c], A. Miller[c]

[a]*Polymer Processing Research Centre, Queen's University, Belfast BT9 5AH, UK*
[b]*School of Chemical Engineering, Queen's University, Belfast BT9 5AG, UK*
[c]*Teleflex Fluid Systems Europe, Kiln Farm, Milton Keynes MK11 3EN, UK*

Received 24 October 2001; received in revised form 20 February 2002; accepted 27 February 2002

Abstract

Blends of a polypropylene (PP) and a metallocene catalysed ethylene–octene copolymer (EOC) were prepared using a single screw extruder fitted with a barrier screw design. The EOC used had 25 wt% 1-octene content and the weight fraction of EOC in the blends covered the range 1–30 wt.% Viscosity values for the blends determined experimentally from dual capillary rheological studies were similar to those calculated theoretically using the log additivity principle described by Ferry. This result together with scanning electron microscopy (SEM) observations and evidence from tan δ curves from dynamic mechanical thermal analysis showed PP and EOC to be partially miscible for blends having 10 wt% EOC or less. The tensile modulus, break strength and flexural modulus of the blends decreased with respect to virgin PP as the weight fraction of EOC was increased to 30 wt.% The diminution in mechanical properties was concomitant with an initial increase in elongation at break from 40% for neat PP to 140% for the blend with 15 wt% EOC before decreasing to 65% when 30 wt% EOC was blended. The optimum impact modification of the PP used in this study, in the temperature range −40 to 23 °C, was achieved by blending with between 20 and 30 wt% EOC.

Keywords: Polypropylene; Ethylene–octene copolymer; Blends

1. Introduction

Polypropylene (PP) is a semi-crystalline polymer [1–3] finding use in a wide variety of industrial applications mainly because of its ease of processing, chemical resistance, low density (typically 0.91 g/cm^3) and relatively low cost. However, its use as an engineering plastic has been limited by its poor impact properties, particularly at low temperatures, due to its high glass transition temperature and relatively high degree of crystallinity. Impact modification and rubber toughening of polypropylene has been a subject of intense research over the last three decades [4–17]. Up to recently, this work has almost exclusively been focused on the incorporation of ethylene–propylene–diene terpolymer (EPDM) [5,6,18–20], ethylene–propylene rubber (EPR) [21–26] and styrene–ethylene/butylene–styrene triblock copolymers (SEBS) [27–32] in PP. Ethylene–vinyl acetate copolymers [33], polybutadiene [34] and natural rubber [35] have also been studied as PP impact modifiers.

Recent developments in constrained geometry metallocene catalyst technology allow copolymers of ethylene and α-olefins to be produced having narrow molecular weight distribution and homogeneous comonomer distribution [36]. The ethylene–octene copolymer (EOC) in particular has been shown to provide a higher toughening contribution than either the ethylene–propylene or ethylene–butene copolymer [37]. Impact modification of both polypropylene homopolymers and copolymers has been achieved with EOC, however the published literature on this topic is limited [38–43]. In this paper we investigate the use of one commercially available EOC (Engage 8150) from DuPont Dow Elastomers as a PP homopolymer impact modifier. We studied the miscibility of PP/EOC blends using rheological, electron microscopy and dynamic mechanical thermal techniques and evaluated the effect of EOC content on the phase morphology, mechanical, impact and thermal properties of the blends prepared.

* Corresponding author. Tel.: +44-28-274-712; fax: +44-28-660-631.
E-mail address: t.mcnally@qub.ac.uk (T. McNally).

0032-3861/02/$ - see front matter
PII: S0032-3861(02)00170-2

2. Experimental

2.1. Materials

The materials used in this study were an isotactic polypropylene (iPP, Novolen 1102J) having a melt flow index of 4.0 g/10 min and a density of 0.91 g/cm^3, supplied by BASF. Engage 8150, a metallocene catalysed copolymer of ethylene and 1-octene (EOC) with 25 wt% of comonomer was provided by DuPont Dow Elastomers with a melt flow index of 0.5 g/10 min and density of 0.868 g/cm^3.

2.2. Blend and test specimen preparation

Blends of PP and EOC containing different weight percent of EOC, 1% ($PP_{99}EOC_1$), 3% ($PP_{97}EOC_3$), 5% ($PP_{95}EOC_5$), 10% ($PP_{90}EOC_{10}$), 15% ($PP_{85}EOC_{15}$), 20% ($PP_{80}EOC_{20}$), 30% ($PP_{70}EOC_{30}$) and 100% (PP) were compounded after tumble mixing using a Killion (Davis Standard) 38 mm diameter extruder fitted with a barrier screw. The temperature profile adopted during compounding of all blends was 165 °C at the feed section increasing to 185 °C for the adapter and die head. Tensile, flexural and impact test specimens were manufactured using an Arburg 320S Allrounder 500–350 injection moulding machine fitted with a 45 mm diameter 18:1 L/D ratio general purpose screw. The temperature profile during moulding was maintained between 200 and 225 °C on going from the feed zone to the nozzle section. All test specimens were allowed to condition under ambient conditions for at least 48 h prior to testing.

2.3. Rheological analysis

The flow properties of the blends were measured using a Rosand dual capillary rheometer (model RH7) with a capillary/die having a 1 mm diameter and length of 16 mm. Data were collected for all blends in the shear rate range 300–4600 s^{-1} at 197, 217 and 237 °C. The instrument was capable of taking measurements at up to 16 different shear rates during one test, and the rheological data obtained were Bagley corrected. Activation energies for flow were calculated using an Arrhenius type expression over the temperature range 197–237 °C. Power law (n) and consistency (K) Indices were calculated from the linear regression of log shear stress versus log shear rate plots. Theoretical viscosities for the blends were calculated, and compared with experimental values, at three constant shear rates, 500, 1000 and 1400 s^{-1}, and three temperatures, 197, 217 and 237 °C, using the log additivity principle described by Ferry [44] to characterise the viscosity of polymer blends:

$$\ln \eta_b = \sum w_i \ln \eta_i \quad (1)$$

where η_b is the viscosity of the blend, and w_i and η_i are, respectively, the weight fraction and viscosity of each component in the blend.

2.4. Mechanical and impact analysis

Tensile tests were performed to ASTM 638 at room temperature (23 °C) using an Instron 4411 Universal tester with a 5 kN load cell and a constant crosshead speed of 200 mm/min. The flexural modulus of the blends was measured to ASTM 790 using the same Instron machine but having a 5 kN compression load cell. Two dimensional impact testing was performed at room temperature (23 °C) and −40 °C using a CEAST automatic fractovis free falling dart impact tester interfaced with a DAS4000 WIN data acquisition system. The peak force (N) and peak energy (J) were recorded and the impact strength calculated by dividing the peak energy by the cross-sectional area of the sample.

2.5. Phase morphology

The morphology of the blends was examined using a JEOL 6400 scanning electron microscope. Samples were cryogenically fractured in liquid nitrogen and etched in heptane at 50 °C for 5 min to extract the elastomeric EOC phase. Samples were coated with gold prior to examination under the electron beam. An operating voltage of 10 kV and a magnification of 3500 was used.

2.6. Thermal analysis

The melting point and relative crystalline content of the blends were determined using a Perkin–Elmer differential scanning calorimeter (model DSC 6) between −120 and 180 °C using a heating and cooling rate of 10 °C/min, under a nitrogen atmosphere. The relative crystallinity of the blends was calculated from the enthalpy value obtained for the melting endotherms of the blends and the enthalpy value for a theoretically 100% crystalline polypropylene (209 J/g) [39,45] taken from literature values. Dynamic mechanical thermal analysis was performed with a Polymer Laboratories DMTA Mark II instrument using specimens of $46 \times 13 \times 3$ mm^3 dimensions in the dual cantilever mode. The samples were examined between −100 and 150 °C at a constant frequency of 1 Hz and a heating rate of 2 °C/min.

3. Results and discussion

3.1. Rheology

The effect of shear rate on the apparent viscosity of the blends was investigated at 197, 217 and 237 °C over the shear rate range 300–4600 s^{-1}. Fig. 1, by way of example, shows the results obtained at 197 °C. The viscosities of both virgin polymers and all the blends decreased as the shear rate increased, indicating pseudoplastic behaviour at 197 °C. Similar behaviour was seen for the measurements at 217 and 237 °C. The viscosity of EOC over the shear rate

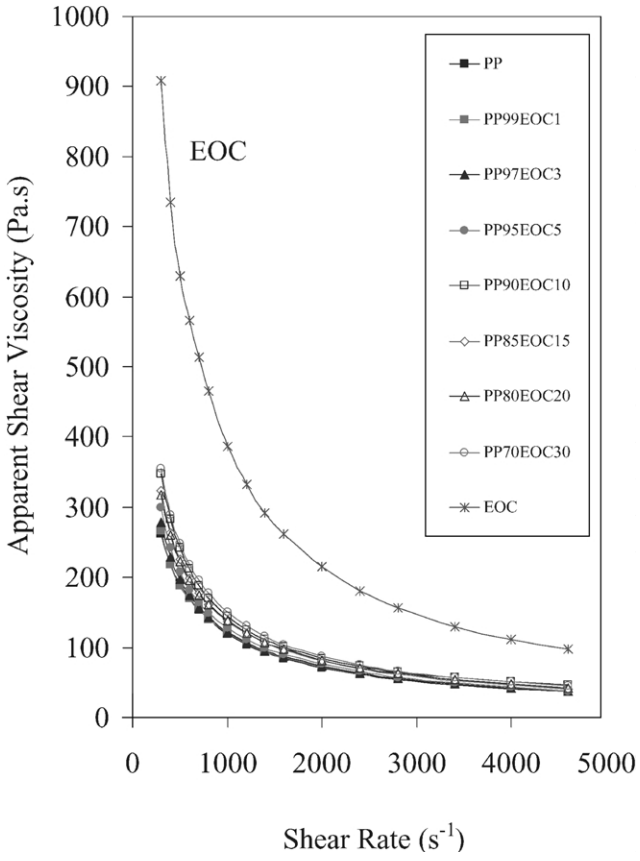

Fig. 1. Shear rate versus shear viscosity for PP, EOC and PP/EOC blends at 197 °C.

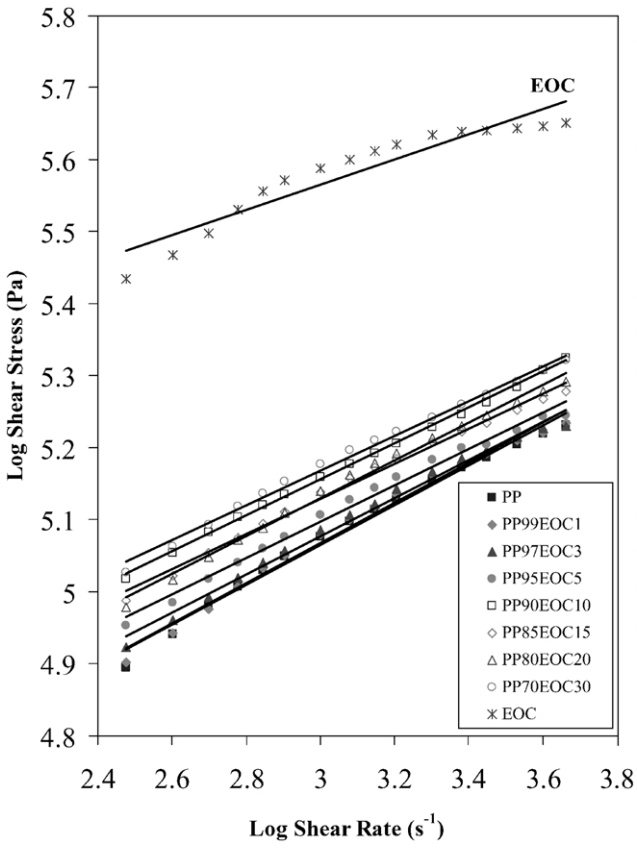

Fig. 2. Log shear rate versus log shear viscosity for PP, EOC and PP/EOC blends at 197 °C.

range investigated is greater than either polypropylene or its blends with EOC. The shear viscosity of the polypropylene increased only slightly on addition of even up to 30 wt% EOC. Power law (n) and consistency (K) indices were determined for all blends from the linear regression of log shear stress versus log shear rate plots, (see Fig. 2 by way of example for data obtained at 197 °C), and together with activation energies for flow calculated using an Arrhenius type expression, are listed in Table 1.

The power law index (n) showed minimal variation with either blend composition or temperature. However, the consistency index (K), which is known to be very temperature sensitive showed greater variation with both shear rate and temperature. Interestingly, K increased with composition as the EOC content in the blends increased to 15 wt% and then fell slightly as the EOC concentration in the blend was increased to 30 wt%. The consistency index (K) decreased for each blend as the temperature of measurement was increased from 197 to 237 °C, the lowest values for both polymers and their blends obtained at 237 °C. Similar results for (n) have been reported by Da Silva et al. [40] for other PP/EOC blends and by Choudhary et al. [46] for

Table 1
Rheological characteristics of PP/EOC blends at 197, 217 and 237 °C

Blend designation	Power law index n			Consistency index K ($\times 10^4$)			Activation energy, E_a (kJ/mol^{-1})
	197	217	237	197	217	237	
PP	0.27	0.31	0.27	2.09	1.35	1.69	8.9
$PP_{99}EOC_1$	0.23	0.32	0.27	2.75	1.33	1.69	10.6
$PP_{97}EOC_3$	0.23	0.30	0.27	2.95	1.55	1.86	10.7
$PP_{95}EOC_5$	0.23	0.28	0.29	2.88	1.68	1.62	10.3
$PP_{90}EOC_{10}$	0.23	0.25	0.28	2.88	2.51	1.69	9.9
$PP_{85}EOC_{15}$	0.23	0.27	0.27	3.31	2.14	1.91	11.2
$PP_{80}EOC_{20}$	0.25	0.29	0.28	2.69	1.82	1.82	10.4
$PP_{70}EOC_{30}$	0.25	0.26	0.29	2.88	2.39	1.78	10.1
EOC	0.17	0.25	0.39	11.75	6.76	1.74	16.3

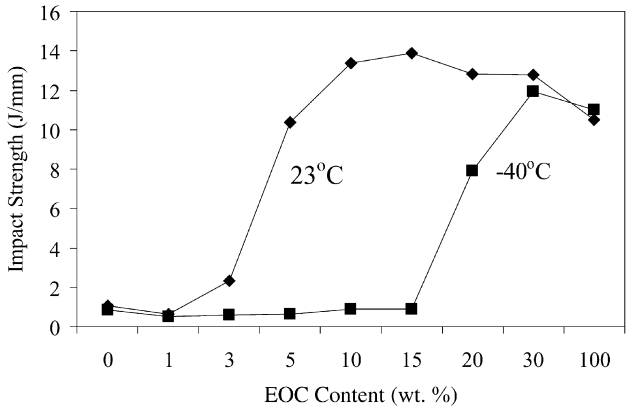

Fig. 3. The effect of composition on the room temperature (23 °C) and cold temperature (−40 °C) impact strength of PP/EOC blends.

polyolefin/rubber blends. The effect of blend composition on activation energy for flow was not significant.

Table 2 lists the experimental, and theoretical viscosity values calculated from Eq. (1). Good agreement was seen between the experimental and theoretical viscosity values obtained for each temperature, and for all three constant shear rates, when the EOC content in the blends was below 15 wt%. The experimental and theoretical values deviated slightly when the EOC content was increased further. This behaviour is consistent, particularly for blends having lower EOC concentrations with a certain degree of miscibility between the PP and EOC phases. As the concentration of the more viscous EOC component is increased in the blend phase separation occurs more readily. Further evidence for partial miscibility between PP and EOC was obtained from DMTA studies and will be discussed in a later section.

3.2. Mechanical and impact properties

The variation in mechanical properties with blend composition is detailed in Table 3. The results showed a decrease in tensile modulus by 41%, break strength by 18% and flexural modulus by 49% with respect to neat PP, as the concentration of EOC in the blend was increased to 30 wt%. The elongation at break increased initially from 40% for this PP to 140% for the blends as the EOC content was increased to 15 wt%, then decreased to 65% as the amount of EOC in the blend was increased further to 30 wt%. The increase in elongation at break obtained for PP/EOC blends relative to virgin PP was concomitant with a significant increase in the impact strength of PP as the concentration of EOC in the blends was increased. Fig. 3 shows the effect of blend composition on the impact strength of PP/EOC blends at room temperature (23 °C) and −40 °C. A rapid increase in impact strength was obtained at room temperature when greater than 5 wt% EOC was added to PP, rising from about 1 J/mm for PP and reaching a plateau at 13.8 J/mm when up to 15 wt% EOC was added. Further addition of EOC up to 30 wt% caused a slight reduction in impact strength to about 11 J/mm. It is interesting to note that the blends $PP_{90}EOC_{10}$, $PP_{85}EOC_{15}$, $PP_{80}EOC_{20}$ and $PP_{70}EOC_{30}$ had greater impact strength at 23 °C than virgin EOC, which had impact strength of 10.5 J/mm. Only a slight increase in impact strength was observed at −40 °C for those blends having a concentration of 15 wt% EOC or less. However, when the loading of EOC in the blends was increased to 20 wt% or above −40 °C impact strength was enhanced significantly, the $PP_{70}EOC_{30}$ blend having similar impact strength (11 J/mm) to virgin EOC. The optimum impact modification of PP in the temperature range −40 to 23 °C was achieved by blending between 20 and 30 wt% EOC with the grade of PP used. Paul and Kale [42] observed similar behaviour for blends in comparable compositions of a PP copolymer with the same EOC used in this study. The improvement in impact strength of the blends with composition may be explained by examining the phase morphology of the blends.

3.3. Morphology of the blends

Fig. 4 shows the scanning electron photomicrographs of the virgin PP and its blends with EOC. Fig. 4(a) and (b) show the cryofractured surface of virgin PP before and after etching in heptane at 50 °C for 5 min. This procedure was adopted to ensure no polymeric component of the PP phase had been etched. The phase morphology after etching, of the $PP_{99}EOC_1$, $PP_{97}EOC_3$, $PP_{95}EOC_5$, $PP_{90}EOC_{10}$ and $PP_{85}EOC_{15}$ blends are displayed in Fig. 4(c)–(g), respectively, and reveal small spherical domains (where EOC had been removed and reflecting the phase morphology of the dispersed phase) dispersed in a PP matrix. The number of domains increased but their average diameter decreased as the concentration of EOC in the blends was increased to 15 wt%. For all blends having up to 15 wt% EOC loading the diameter of the domains never exceeded 1 μm. The smallest average domain diameter, between 0.15 and 0.60 μm was seen for the $PP_{85}EOC_{15}$ blend. This diameter size is typical for what has been reported previously for both PP/EOC and PE/EOC blends [47,48] and is in the range required to toughen blends where the matrix polymer is ductile [4]. As the concentration of EOC was increased further to 20 and 30 wt% the dispersed phase had transformed from a spherical like domain to a more elongated feature. The optimum percentage elongation at break and improved impact properties obtained for the blends having an EOC concentration of 15 wt% or greater may arise as a consequence of the spherical and slightly elongated (distorted spherical) phase morphology of the elastomeric EOC being well dispersed in the PP matrix. The very few domains evident for the $PP_{99}EOC_1$ and $PP_{97}EOC_3$ blends may perhaps indicate a certain degree of miscibility between the PP and EOC at these low EOC loadings in the blends. No cocontinuous phase morphology was evident

Table 2
Experimental and theoretical viscosities for PP, EOC and PP/EOC blends at 197, 217 and 237 °C and three different shear rates, 500, 1000 and 1400 s^{-1}

Blend	Shear rate γ (s^{-1})	197 °C		217 °C		237 °C	
		Apparent viscosity η (Pa s)	Theoretical viscosity $\ln \eta_b = \sum w_i \ln \eta_i$	Apparent viscosity η (Pa s)	Theoretical viscosity $\ln \eta_b = \sum w_i \ln \eta_i$	Apparent viscosity η (Pa s)	Theoretical viscosity $\ln \eta_b = \sum w_i \ln \eta_i$
PP	500	222		191		183	
	1000	135		119		112	
	1400	103		93		88	
$PP_{99}EOC_1$	500	239	225	189	194	187	185
	1000	139	136	120	121	114	113
	1400	108	104	94	94	89	89
$PP_{97}EOC_3$	500	244	230	197	198	192	187
	1000	143	139	122	124	116	115
	1400	110	106	95	96	90	90
$PP_{95}EOC_5$	500	245	235	208	203	191	190
	1000	142	142	128	127	117	116
	1400	110	109	100	98	92	92
$PP_{90}EOC_{10}$	500	243	249	242	215	194	198
	1000	142	150	144	135	119	121
	1400	110	114	111	104	93	96
$PP_{85}EOC_{15}$	500	269	264	227	229	203	205
	1000	156	159	137	143	124	126
	1400	120	121	106	110	96	100
$PP_{80}EOC_{20}$	500	258	279	223	243	208	213
	1000	153	167	138	152	127	131
	1400	118	127	108	117	99	104
$PP_{70}EOC_{30}$	500	274	314	248	273	215	230
	1000	161	187	151	170	132	142
	1400	125	141	116	131	105	114
EOC	500	702		629		390	
	1000	397		387		250	
	1400	295		292		206	

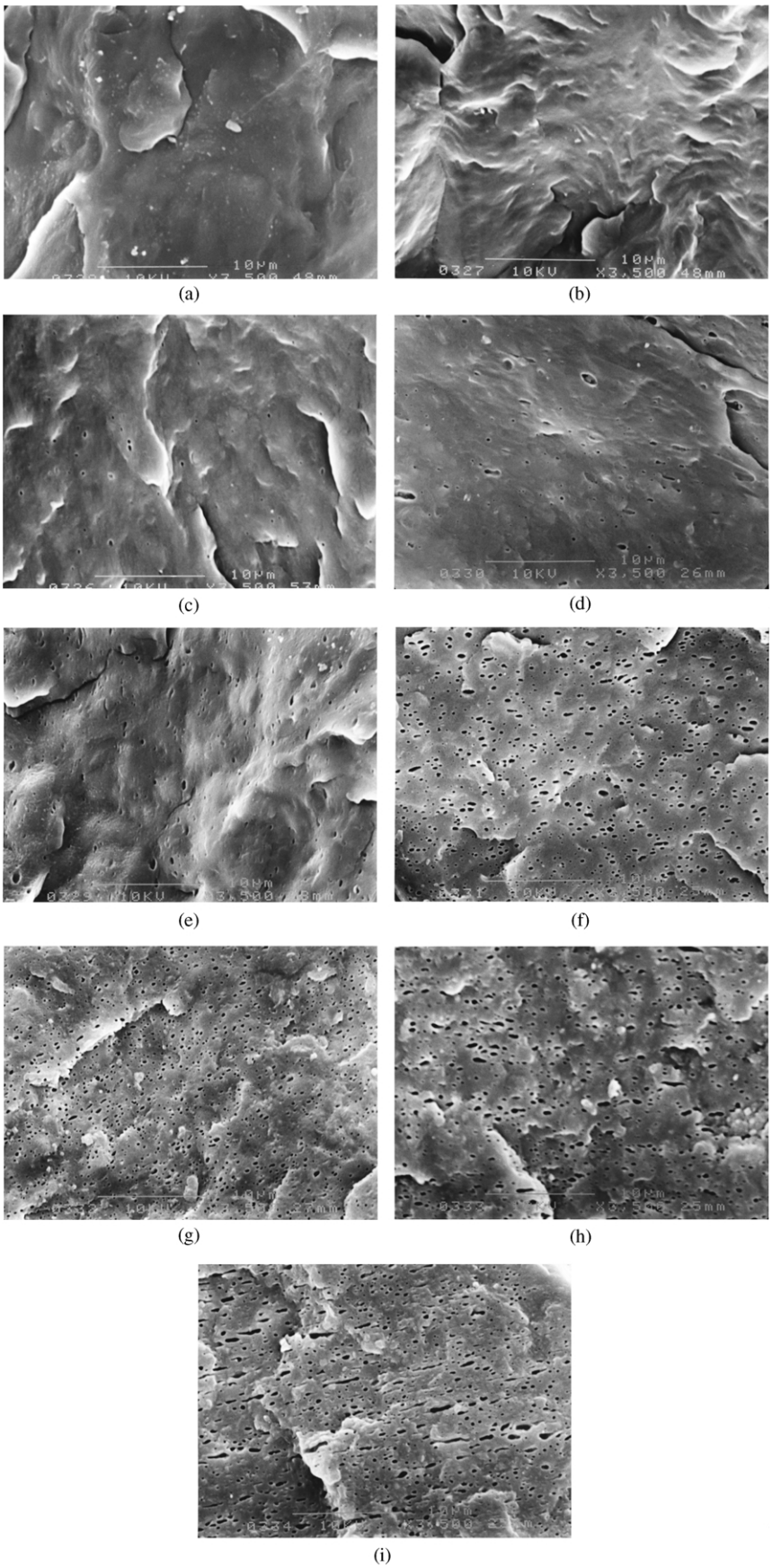

Fig. 4. SEM photomicrographs of (a) PP unetched, (b) PP etched in heptane at 50 °C for 5 min, and the blends, (c) $PP_{99}EOC_1$, (d) $PP_{97}EOC_3$, (e) $PP_{95}EOC_5$, (f) $PP_{90}EOC_{10}$, (g) $PP_{85}EOC_{15}$, (h) $PP_{80}EOC_{20}$ and (i) $PP_{70}EOC_{30}$.

Table 3
Mechanical properties of PP/EOC blends

Blend	Tensile modulus (MPa)	Break strength (MPa)	Flexural modulus (MPa)	Elongation at break (%)
PP	964	19.5	1336	39.5
$PP_{99}EOC_1$	901	19.0	1301	39.9
$PP_{97}EOC_3$	899	16.2	1241	57.8
$PP_{95}EOC_5$	879	18.0	1287	83.3
$PP_{90}EOC_{10}$	774	17.1	1117	115.7
$PP_{85}EOC_{15}$	739	16.8	1027	140.7
$PP_{80}EOC_{20}$	675	17.6	874	88.7
$PP_{70}EOC_{30}$	564	15.9	681	65.3
EOC	6	5.0	9	672.9

for the blends studied, perhaps either the low concentration of EOC in the blends or the cryofractured surfaces not facilitating a co-continuous morphology to develop.

3.4. Thermal analysis

Fig. 5 shows the DSC heating curves only for PP, EOC and blends of PP/EOC over the temperature range −100 to 180 °C and Table 4 lists the DSC characteristics of both virgin polymers and their blends. PP itself displayed one feature, a sharp endothermic melting process at 168 °C, in contrast to the EOC which had a broad crystalline melting feature between 25 and 80 °C having a peak maximum at 36 °C, and a glass transition at about −50 °C. The DSC traces of all the blends revealed a clearly resolved melting endotherm associated with the PP rich phase with similar peak maxima to that obtained for PP itself, suggesting that lamellae thickness is independent of blend composition. There was a slight broadening of the melting endotherm for the blends with increasing EOC concentration, reflecting a distribution of PP crystallite size and perfection as a consequence of the disruption of the PP crystal morphology by the EOC. The percentage crystallinity of the PP was calculated from the ratio of the enthalpy of fusion for the blend and the enthalpy of fusion for a theoretically 100% crystalline PP, taken as 209 J/g, and adjusted for the nominal mass fraction of PP in the blend. As may be seen from Table 4 the crystalline content of the blends decreased from 39 to 34% as the EOC content in the blends was increased to 30 wt%. It is difficult to assess the significance of this slight reduction in crystallinity of the blends, as the variation observed is most probably within experimental error of the instrument. Further thermal analyses of the glass transition processes of the blends, perhaps using modulated differential scanning calorimetry (MDSC), might elucidate the extent of miscibility of PP/EOC blends, particularly at lower EOC concentrations [49]. The melting process associated with the EOC rich phase was not evident in the DSC curves for the blends with 5 wt% EOC or less, but became better resolved as the EOC content in the blends was increased further.

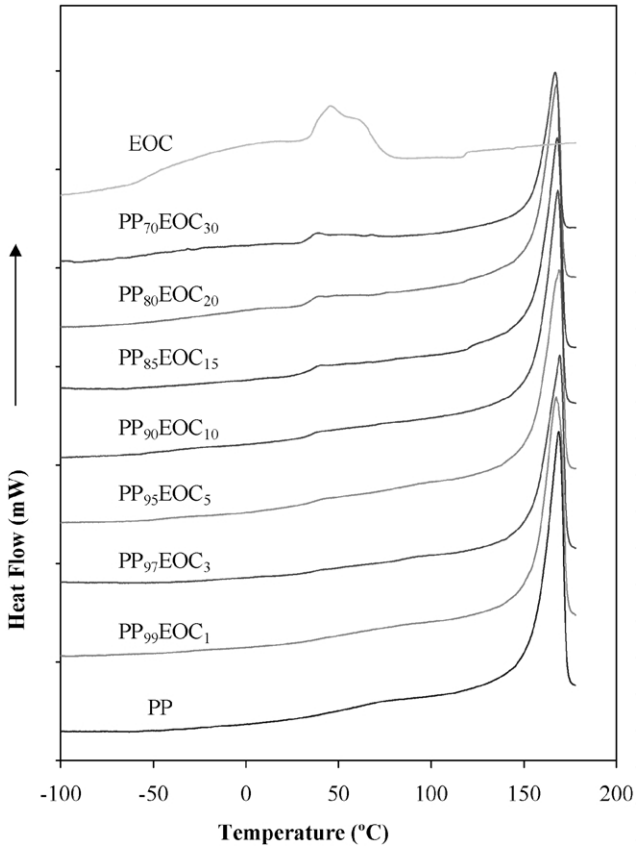

Fig. 5. DSC traces of PP, EOC and PP/EOC blends.

The variation in tan δ and storage modulus (E') as function of temperature for PP, EOC and their blends are shown in Figs. 6 and 7. The tan δ curve for EOC alone shows one

Table 4
DSC characteristics of PP/EOC blends

Blend	T_m (°C)	ΔH (J/g)	ΔH (J/g)/wt% PP	% Crystallinity
PP	168	82.2	82.2	39.3
PP99EOC1	167	82.6	83.5	39.9
PP97EOC3	169	76.2	78.6	37.6
PP95EOC5	169	74.7	78.6	37.6
PP90EOC10	168	70.1	77.9	37.3
PP85EOC15	168	66.6	78.4	37.5
PP80EOC20	168	57.0	71.3	34.1
PP70EOC30	167	49.4	70.5	33.7
EOC	46	32.6	–	–

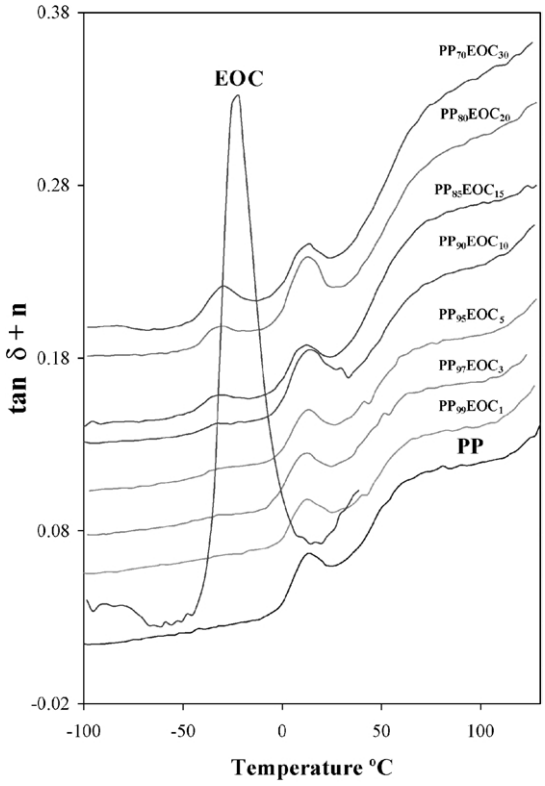

Fig. 6. Variation in tan δ as a function of temperature for PP, EOC and PP/EOC blends.

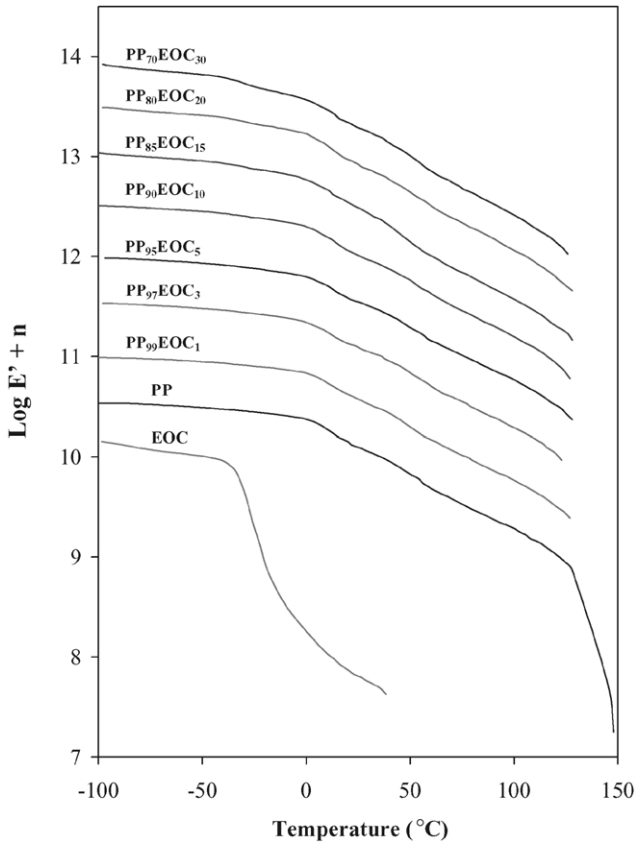

Fig. 7. Variation in storage modulus (E') as a function of temperature for PP, EOC and PP/EOC blends.

sharp intense peak at −20 °C associated with the glass transition process of EOC. One clearly resolved peak was also evident for PP itself in the temperature range examined, centred at about 15 °C and derived from the glass transition of the PP amorphous phase. The tan δ curves for the blends having 1, 3 and 5 wt% EOC exhibited only one feature attributed to the glass transition of the PP phase. When the EOC concentration was increased to between 10 and 30 wt% two processes were observed. Firstly, as with those blends having 5 wt% EOC or less, a peak attributed to the glass transition of PP was present, and secondly a feature at lower temperatures which became better resolved with increased EOC content, associated with the glass transition of the EOC phase. The presence of just one peak in the blends consisting of 1, 3 and 5 wt% and perhaps the 10 wt% blend (as the process in question is poorly resolved), the shifting of the peak maximum of the EOC glass transition to lower temperatures and the significant reduction of the peak intensity would suggest that EOC is miscible with the PP, particularly at lower EOC content in the blends. A certain degree of interaction between PP and EOC also occurs at EOC concentrations above 10 wt%. This result is consistent with our observations from the rheological and electron microscopy studies of the blends. The storage modulus of EOC below its glass transition temperature (−20 °C) was about 1.5 orders of magnitude greater than either PP itself or any PP/EOC blend. The storage modulus of the blends above the glass transition of the EOC phase in the temperature range studied decreased as the concentration of EOC in the blends was increased. All the blends persisted within the measurement system to about 140 °C, the temperature at which the PP crystallites started to melt and the blends began to flow.

4. Conclusions

Blends of polypropylene and a metallocene catalysed ethylene–octene copolymer were successfully prepared using a single-screw extruder fitted with a barrier screw. Yu reported similar processing equipment to be effective compounders for other polypropylene ethylene α-olefin copolymer blends [50].

Rheology data, scanning electron microscopy observations and tan δ curves from DMTA measurements showed PP and EOC to be miscible for the blends having up to 10 wt% EOC ($PP_{90}EOC_{10}$), and perhaps as high as 15 wt% ($PP_{85}EOC_{15}$). The tensile modulus, break strength and flexural modulus of the blends decreased with respect to virgin PP as the concentration of EOC in the blends was increased to 30 wt%. Conversely, the elongation at break increased initially from 40% for neat PP to 140% for the $PP_{85}EOC_{15}$ blend, before decreasing to 65% with further successive additions of EOC up to 30 wt%.

Significant improvements in impact properties of virgin PP were obtained at both room temperature when 10 wt% EOC was added ($PP_{90}EOC_{10}$), and at −40 °C when 25 wt% EOC or greater was blended. The optimum impact modification of the PP used in this study in the temperature range −40 to 23 °C was achieved by blending with between 20 and 30 wt% EOC.

Acknowledgements

The authors would like to acknowledge DuPont Dow Elastomers for providing Engage 8150, Stephen McFarland and Jacqueline Patrick (Electron Microscopy Unit, Queen's University, Belfast) for their assistance in producing the electron photomicrographs, and Neil Callan for computing assistance.

References

[1] Lotz B, Wittmann JC, Lovinger AJ. Polymer 1996;37:4979.
[2] Varga J. J Mater Sci 1992;27:2557.
[3] Jacoby P, Bersted BH, Kissel WJ, Smith CE. J Polym Sci Part B: Polym Phys 1986;24:461.
[4] Bucknall CB. Toughened plastics. London: Applied Science, 1977.
[5] Ho WJ, Salovev R. Polym Engng Sci 1981;21:839.
[6] D'Oragio L, Greco R, Martuscelli E, Ragosta G. Polym Engng Sci 1983;23:489.
[7] Dao KC. Polymer 1984;25:1527.
[8] van der Ven S. Polypropylene and other polyolefins: polymerisation and characterisation. Amsterdam: Elsevier, 1990.
[9] Karger-Kocsis J, editor. Polypropylene: structures, blends and composites. London: Chapman & Hall, 1995.
[10] Inoue T, Suzuki T. J Appl Polym Sci 1996;59:1443.
[11] Mouzakis DE, Gahleitner M, Karger-Kocsis J. J Appl Polym Sci 1998;70:837.
[12] Yokoyama Y, Ricco T. Polymer 1998;39:3675.
[13] van der Wal A, Mulder JJ, Oderkerk J, Gaymans RJ. Polymer 1998; 39:6781.
[14] van der Wal A, Mighof R, Gaymans RJ. Polymer 1999;40:6045.
[15] van der Wal A, Mighof R, Gaymans RJ. Polymer 1999;40:6057.
[16] van der Wal A, Mighof R, Gaymans RJ. Polymer 1999;40:6087.
[17] Liang JZ, Li RKY. Polymer 2000;77:409.
[18] Stehling FC, Huff T, Speed CS, Wissler G. J Appl Polym Sci 1981;26: 2693.
[19] D'Oragio L, Greco R, Manearella E, Ragosta G, Silvestre C. Polym Engng Sci 1982;22:536.
[20] Duvdevani I, Agarwal PF, Lundberg RD. Polym Engng Sci 1982; 22:499.
[21] Danesi S, Porter RS. Polymer 1978;19:448.
[22] Galli P, Danesi S, Simonazzi T. Polym Engng Sci 1984;24:544.
[23] Ito J, Mitani K, Mizutani Y. J Appl Polym Sci 1984;29:75.
[24] Yang D, Zhang B, Yang Y, Fang Z, Sun G, Feng Z. Polym Engng Sci 1984;24:612.
[25] Chiu WY, Fang SJ. J Appl Polym Sci 1985;30:1473.
[26] Greco R, Manearella G, Martuscelli E, Ragosta G, Jinghua Y. Polymer 1987;28:1929.
[27] Gupta AK, Punwar SN. J Appl Polym Sci 1984;29:1079.
[28] Gupta AK, Punwar SN. J Appl Polym Sci 1984;29:1595.
[29] Gupta AK, Punwar SN. J Appl Polym Sci 1984;29:3513.
[30] Gupta AK, Punwar SN. J Appl Polym Sci 1985;30:1777.
[31] Gupta AK, Punwar SN. J Appl Polym Sci 1985;30:1799.
[32] Gupta AK, Punwar SN. J Appl Polym Sci 1986;31:535.
[33] Jafari SH, Gupta AK. J Appl Polym Sci 2000;78:962.
[34] Gupta AK, Ratnam BK. J Appl Polym Sci 1991;42:297.
[35] Yoon LK, Choi CH, Kim BK. J Appl Polym Sci 1995;56:239.
[36] Kaminsky W. Macromol Chem Phys 1996;197:3907.
[37] Sylvest RT, Lancester G, Betso SR. Kautschuk Gummi Kunststoffe 1997;50:186.
[38] Dharmarajan NR, Yu TC. Plast Engng 1996;52:33.
[39] Da Silva ALN, Tavares MIB, Politano DP, Coutihno FMB, Rocha MCG. J Appl Polym Sci 1997;66:2005.
[40] Da Silva ALN, Rocha MCG, Coutinho FMB, Bretas R, Scuracchio C. Polym Test 2000;19:363.
[41] Da Silva ALN, Rocha MCG, Coutihno FMB, Bretas R, Scuracchio C. J Appl Polym Sci 2000;75:692.
[42] Paul S, Kale DD. J Appl Polym Sci 2000;76:1480.
[43] Da Silva ALN, Rocha MCG, Coutihno FMB, Bretas RES, Scuracchio C. J Appl Polym Sci 2001;79:1634.
[44] Ferry JD. Viscoelastic properties of polymers. New York: Wiley, 1970.
[45] van Krevelen DW, Hoftyzer PJ. Properties of polymers, their estimation and correlation with chemical structure. New York: Elsevier, 1976.
[46] Choudhary V, Varma HS, Varma IK. Polymer 1991;32:2541.
[47] Premphet K, Paecharoenchai W. J Appl Polym Sci 2001;82:2140.
[48] Kukaleva N, Jollands M, Cser F, Kosior E. J Appl Polym Sci 2000;76: 1011.
[49] Kukaleva N, Cser F, Jollands M, Kosior E. J Appl Polym Sci 2000;77: 1591.
[50] Yu TC. Proc SPE ANTEC 1996;42:1995.